

Testing the Randomness in the Sky-Distribution of Gamma-Ray Bursts

R. Vavrek,¹ * L. G. Balázs,² A. Mészáros,³ I. Horváth⁴ and Z. Bagoly⁵

¹*ESA/ESAC P.O. Box 50727 Villafranca del Castillo, 28080 Madrid, Spain*

²*Konkoly Observatory, P. O. Box 67, H-1525 Budapest, Hungary*

³*Astronomical Institute of the Charles University, V Holešovičkách 2, 180 00 Prague 8, Czech Republic*

⁴*Department of Physics, Bolyai Military University, P. O. Box 15, H-1581 Budapest, Hungary*

⁵*Laboratory for Information Technology, Eötvös University, Pázmány Péter sétány 1/A, H-1518 Budapest, Hungary*

Accepted XXXX ... XX. Received XXXX ... XX; in original form XXXX ... XX

ABSTRACT

We studied the complete randomness of the angular distribution of gamma-ray bursts (GRBs) detected by BATSE. Since GRBs seem to be a mixture of objects of different physical nature we divided the BATSE sample into 5 subsamples (short1, short2, intermediate, long1, long2) based on their durations and peak fluxes and studied the angular distributions separately. We used three methods, Voronoi tessellation, minimal spanning tree and multifractal spectra to search for non-randomness in the subsamples. To investigate the eventual non-randomness in the subsamples we defined 13 test-variables (9 from the Voronoi tessellation, 3 from the minimal spanning tree and one from the multifractal spectrum). Assuming that the point patterns obtained from the BATSE subsamples are fully random we made Monte Carlo simulations taking into account the BATSE's sky-exposure function. The MC simulations enabled us to test the null hypothesis i.e. that the angular distributions are fully random. We tested the randomness by binomial test and introducing squared Euclidean distances in the parameter space of the test-variables. We concluded that the short1, short2 groups deviate significantly (99.90%, 99.98%) from the fully randomness in the distribution of the squared Euclidean distances but it is not the case at the long samples. At the intermediate group the squared Euclidean distances also give significant deviation (98.51%).

1 INTRODUCTION

Recently, there is no doubt about the cosmological origin of the gamma-ray bursts (hereafter GRBs) (Zhang & Mészáros 2004; Fox et al. 2005; Mészáros 2006). Then, assuming a large scale isotropy for the Universe, one expects the same property for the GRBs as well. Another property, which is also expected to occur that GRBs should appear fully randomly, i.e. if a burst is observed it does not give any information about the place of the next one. If both properties are fulfilled, then the distribution is called completely random (for the astronomical context of spatial point processes see Pásztor & Tóth (1995)). There are several tests for checking the complete randomness of point patterns, however, these procedures do not always give information for both properties simultaneously.

There are increasing evidence that all the GRBs do not represent a physically homogeneous group (Kouveliotou et al. 1993; Horváth 1998; Mukherjee et al. 1998; Hakkila et al. 2000; Horváth 2002; Balázs et al. 2003; Hakkila et al. 2003; Horváth et al. 2006). Hence, it is worth investigating that the physically different subgroups are also different in their angular distributions. In the last years the authors provided (Balázs et al. 1998, 1999; Mészáros et al. 2000a,b) several different tests probing the intrinsic isotropy in the angular sky-distribution of GRBs collected in BATSE Catalog (Meegan et al. 2000). Shortly summarizing the results of these studies one may conclude: A. The long subgroup ($T_{90} > 10$ s) seems to be distributed isotropically; B. The intermediate subgroup (2 s $\leq T_{90} \leq 10$ s) is distributed anisotropically on the $\simeq (96 - 97)\%$ significance level; C. For the short subgroup (2 s $> T_{90}$) the assumption of isotropy is rejected only on the 92% significance level; D. The long and the short subclasses, respectively, are distributed differently on the 99.3% significance level. (About the definition of subclasses see Horváth (1998); T_{90} is the duration of a GRB, during which time the 90% of the radiated energy is received (Meegan et al. 2000).)

Independently and by different tests, Litvin et al. (2001) confirmed the results A., B. and C. with one essential difference: for the intermediate subclass a much higher - namely 99.89% - significance level of anisotropy is claimed. Again, the short subgroup is found to be "suspicious", but only the $\simeq (85 - 95)\%$ significance level is reached. The long subclass seems to be distributed isotropically (but see Mészáros & Štoček (2003)). Magliocchetti et al. (2003) found significant angular correlation on the $2^\circ - 5^\circ$ scale for GRBs with $T_{90} < 2$ s durations. Tanvir et al. (2005) reported a correlation between the locations of previously observed short

bursts and the positions of galaxies in the local Universe, indicating that between 10 and 25 per cent of short GRBs originate at low redshifts ($z < 0.025$).

It is a reasonable requirement to continue these tests using more sophisticated procedures in order to see whether the angular distribution of GRBs is completely random or has some sort of regularity. This is the subject of this article. New tests will be presented here. Mainly the clarification of the short subgroup's behaviour is expected from these tests. In this paper, similarly to the previous studies, the *intrinsic* randomness is tested; this means that the non-uniform sky-exposure function of BATSE instrument is eliminated.

The paper is organized as follows. In Section 2 the three new tests are described. This Section does not contain new results, but - because the methods are not widely familiar - this minimal survey may be useful. Section 3 contains the statistical tests on the data. Section 4 summarizes the results of the statistical tests, and Section 5 presents the main conclusions of the paper.

2 MATHEMATICAL SUMMARY

2.1 Voronoi tessellation (VT)

The Voronoi diagram - also known as Dirichlet tessellation or Thiessen polygons - is a fundamental structure in computational geometry and arises naturally in many different applications (Voronoi 1908; Stoyan & Stoyan 1994). Generally, this diagram provides a partition of a point pattern ("point field", also "point process") according to its spatial structure, which can be used for analyzing the underlying point process.

Assume that there are N points ($N \gg 1$) scattered on a sphere surface with an unit radius. One says that a point field is given on the sphere. The Voronoi cell (Stoyan & Stoyan 1994) of a point is the region of the sphere surface consisting of points which are closer to this given point than to any other ones of the sphere. This cell forms a polygon on this sphere. Every such cell has its area (A) given in steradian, perimeter (P) given by the length of boundary (one great circle of the boundary curve is called also as "chord"), number of vertices (N_v) given by an integer positive number, and by the inner angles (α_i ; $i = 1, \dots, N_v$). This method is completely non-parametric, and therefore may be sensitive for various point pattern structures in the different subclasses of GRBs.

Note that the behaviour of this tessellation method on the sphere surface is quite different from that on the infinite plane. This follows from the fact that the polygon's area will not be

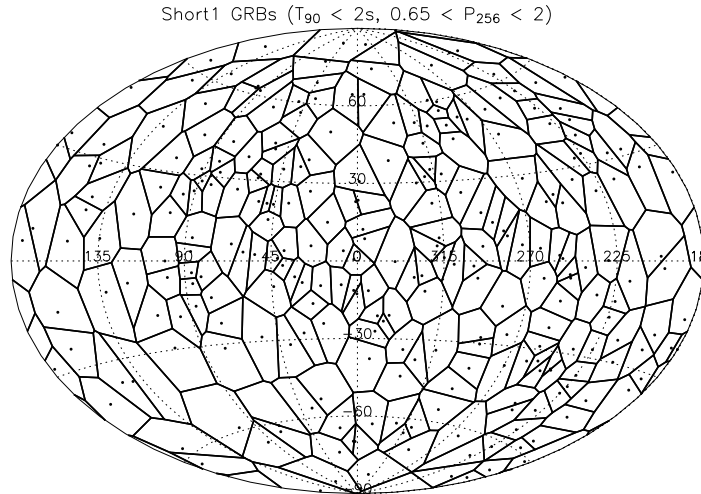


Figure 1. Voronoi tessellation of the short GRBs (Short1 sample) in the $0.65 < P_{256} < 2.00$ peak-flux range in Galactic coordinates. The peak-flux is given in dimension $\text{photon}/(\text{cm}^2\text{s})$.

independent from each other, because the total surface of the sphere is fixed in 4π steradian. Hence, the spherical Voronoi tessellation is not effected by border effects, and the Voronoi diagram becomes a closed set of convex polygons.

The points on sphere may be distributed completely randomly or non-randomly; the non-random distribution may have different characters (clustering, filaments, etc.; for the survey of these non-random behaviours see, e.g., Diggle (1983)).

Random and some regular patterns have distributions of one characteristic maxima (unimodal) but with different variances. The multimodality means different characteristic maxima indicating hierarchical (cluster) structure, the number of modes is determined by the number of scales in the sample. The VT method is able both to detect the non-randomness and to describe its form (for more details see Stoyan & Stoyan (1994) and for the astronomical context Coles & Barrow (1990); Coles (1991); Icke & van de Weygaert (1991); Ikeuchi & Turner (1991); Subba Rao & Szalay (1992); van de Weygaert (1994); Zaninetti (1995); Doroshkevich et al. (1997); Yahagi et al. (1999); Ramella et al. (2001)).

2.2 Minimal spanning tree (MST)

Contrary to VT, this method considers the distances (edges) among the points (vertices). Clearly, there are $N(N-1)/2$ distances among N points. A spanning tree is a system of lines connecting all the points without any loops. The minimal spanning tree (MST) is a system of connecting lines, where the sum of the lengths is minimal among all the possible connections

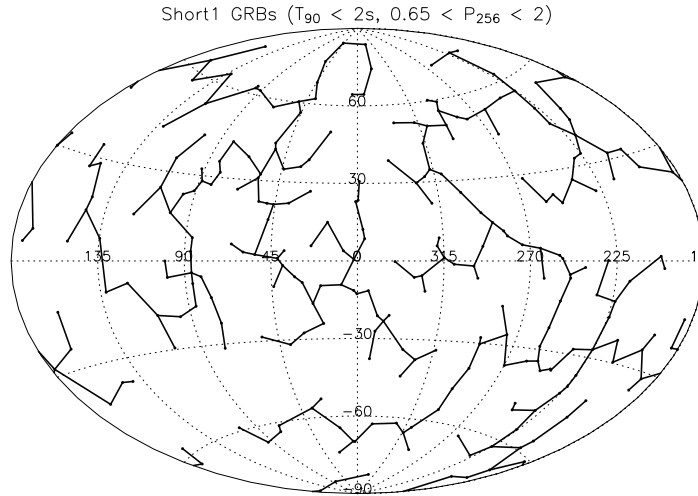


Figure 2. The MST for the sample in Fig.1.

between the points (Kruskal 1956; Prim 1957). In this paper the spherical version of MSF is used following the original Prim’s paper.

The $N - 1$ separate connecting lines (edges) together define the minimal spanning tree. The statistics of the lengths and the α_{MST} angles between the edges at the vertices can be used for testing the randomness of the point pattern. The MST is widely used in cosmology for studying the statistical properties of galaxy samples (Barrow et al. 1985; Bhavsar & Lauer 1996; Krzewina & Saslaw 1996; Bhavsar & Splinter 1996; Adami & Mazure 1999; Doroshkevich & Turchaninov 2001).

2.3 Multifractal spectrum

Let denote $P(\varepsilon)$ the probability for finding a point in an area of ε radius. If $P(\varepsilon)$ scales as ε^α (i.e. $P(\varepsilon) \propto \varepsilon^\alpha$), then α is called the local fractal dimension (e.g. $\alpha = 2$ for a completely random process on the plane). In the case of a monofractal α is independent on the position. A multifractal (MFR) on a point process can be defined as unification of the subsets of different (fractal) dimensions (Paladin & Vulpiani 1987). One usually denotes with $f(\alpha)$ the fractal dimension of the subset of points at which the local fractal dimension is in the interval of $\alpha, \alpha + d\alpha$. The contribution of these subsets to the whole pattern is not necessarily equally weighted, practically it depends on the relative abundances of subsets. The $f(\alpha)$ functional relationship between the fractal dimension of subsets and the corresponding local fractal dimension is called the MFR or Hausdorff spectrum.

In the vicinity of i -th point ($i = 1, 2, \dots, N$) one can measure from the neighbourhood

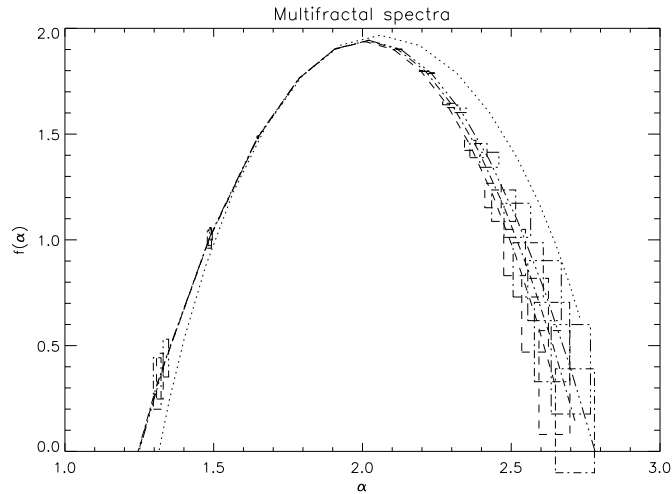


Figure 3. MFR spectra of simulated (dot-dashed), Long1 (dashed), Short1 (dotted) and Short2 (three-dot-dashed) samples. Boxes represent the error of spectrum points derived from Monte Carlo simulations. Note the shift of the maximum of the spectrum of the Short1 sample towards higher values in comparison to $\alpha = 2$, corresponding to the completely random 2D Euclidean case.

structure a local dimension α_i ("Rényi dimension"). This measure approximates the dimension of the embedding subset, giving a possibility to construct the MFR spectrum which characterizes the whole pattern (for more details see Paladin & Vulpiani (1987)). If the maximum of this convex spectrum is equal to the Euclidean dimension of the space, then in classical sense the pattern *is not a fractal*, but the spectrum remains sensitive to the non-randomness of the point set.

There is a wide variety of astronomical phenomena, where the concept of fractal and/or multifractal can be successfully applied (Giraud 2000; Irwin et al. 2000; Kawaguchi et al. 2000; Pan & Coles 2000; Selman & Melnick 2000; Bottorff & Ferland 2001; Célérier & Thieberger 2001; Chappell & Scalo 2001; Tatekawa & Maeda 2001; Vavrek et al. 2001; Aschwanden & Parnell 2002; Casuso & Beckman 2002; Elmegreen 2002; Gaité & Manrubia 2002; Pan & Coles 2002; Semelin & Combes 2002; Tikhonov 2002; Datta 2003).

3 STATISTICAL TESTS ON THE DATA

The three procedures outlined in Section 2 enable us to derive several stochastic quantities well suited for testing the non-randomness of the underlying point patterns.

3.1 Input data and the definition of samples

Up to the present the most comprehensive all-sky survey of GRBs was done by the BATSE experiment on board of the CGRO satellite in the period of 1991-2000. In this period the

Table 1. Tested samples of BATSE GRBs.

Sample	Duration [s]	Peak flux [photons $cm^{-2}s^{-1}$]	Number of GRBs
Short1	$T_{90} < 2$ s	$0.65 < P_{256} < 2$	261
Short2	$T_{90} < 2$ s	$0.65 < P_{256}$	406
Intermediate	$2 \text{ s} \leq T_{90} \leq 10 \text{ s}$	$0.65 < P_{256}$	253
Long1	$T_{90} > 2$ s	$0.65 < P_{256} < 2$	676
Long2	$T_{90} > 10$ s	$0.65 < P_{256}$	966

experiment collected 2704 well justified burst events and the data are available in the Current BATSE Catalog (Meegan et al. 2000).

Since there are increasing evidence (Horváth et al. (2006) and references therein) that the GRB population is actually a mixture of astrophysically different phenomena, we divided the GRBs into three groups: *short* ($T_{90} < 2s$), *intermediate* ($2s \leq T_{90} \leq 10s$) and *long* ($T_{90} > 10s$). To avoid the problems with the changing detection threshold we omitted the GRBs having a peak flux $P_{256} \leq 0.65 \text{ photons } cm^{-2} s^{-1}$. This truncation was proposed by Pendleton et al. (1997). The bursts may emerge at very different distances in the line of sight and it may happen that the stochastic structure of the angular distribution depends on it. Therefore, we also made tests on the bursts with $P_{256} < 2 \text{ photons } cm^{-2} s^{-1}$ in the short and long population, separately. Table 1 defines the 5 samples to be studied here.

3.2 Definition of the test-variables

The randomness of the point field on the sphere can be tested with respect to different criteria. Since different non-random behaviours are sensitive for different types of criteria of non-randomness, it is not necessary that all possible tests using different measures reject the assumption of randomness. In the following we defined several test-variables which are sensitive to different stochastic properties of the underlying point pattern, as proposed by Wallet & Dussert (1998).

3.2.1 Voronoi tessellation

Any of the four quantities characterizing the Voronoi cell, i.e. the area, the perimeter, the number of vertices, and the inner angles can be used as test-variables or even some of their combinations, too. We defined the following test-variables:

- Cell area A ;
- Cell vertex (edge) N_v ;

- Cell chords C ;
- Inner angle α_i ;
- Round factor (RF) average $RF_{av} = \overline{4\pi A/P}$;
- Round factor (RF) homogeneity $1 - \frac{\sigma(RF_{av})}{RF_{av}}$;
- Shape factor A/P^2 ;
- Modal factor $\sigma(\alpha_i)/N_v$;
- The so-called "AD factor" defined as $AD = 1 - (1 - \sigma(A)/\langle A \rangle)^{-1}$, where $\sigma(A)$ is the dispersion and $\langle A \rangle$ is the average of A .

3.2.2 Minimal spanning tree

To characterize the stochastic properties of a point pattern we use three quantities obtained from a MST:

- Variance of the MST edge-length $\sigma(L_{MST})$;
- Mean MST edge-length L_{MST} ;
- Mean angle between edges α_{MST} .

3.2.3 Multifractal spectrum

Here the only used variable is the $f(\alpha)$ multifractal spectrum, which is a sensitive tool for testing the non-randomness of a point pattern.

An important problem is to study the sensitivity (discriminant power) of the different parameters to the different kind of regularity inherent in the point pattern. In the case of a fully regular mesh, e.g., A is constant and so $AD = 0$, $\sigma(\alpha_i) = 0$ and both are increasing towards a fully random distribution. In case of a patchy pattern the distribution of the area of the Voronoi cells and the edge distribution of MST become bimodal reflecting the average area and edge length within and between the clusters, in comparison to the fully random case. In a filamentary distribution the shape of the areas becomes strongly distorted reflecting in an increase of the modal factor in comparison to the case of patches.

Wallet & Dussert (1997) investigated the power of the Voronoi tessellation and minimal spanning tree in discriminating between distributions having big and small clusters, full randomness and hard cores (random distributions but the mutual distances of the points are constrained by the size of a hard core), respectively. They concluded that Voronoi roundness factor did not separate small clusters and hardcore distributions, and roundness factor

homogeneity did not distinguish between small clusters and random distributions, **nor** between random and hardcore distributions. MST has a very good discriminant power even in the case of hardcore distributions with close minimal interpoint distances.

Since the sensitivity of the variables are different on changing the regularity properties of the underlying point patterns one may measure significant differences in one parameter but not in the other even in the case when these are correlated otherwise. It is not a trivial issue. In most cases one needs extended numerical simulations to study the statistical significance of the different parameters.

3.3 Estimation of the significance

Let us denote with ξ one of the thirteen test-variables defined in Section 3.2. The probability that $\xi < x$ occurs is given by $P(\xi < x) = F(x)$, where $F(x)$ is the probability distribution function. We approximated $F(x)$ numerically by the $F_n(x)$ empirical probability distribution function which can be calculated by $F_n(x) = k/n$ where n is the number of simulations and k is the number of cases for which the simulated $\xi < x$ holds.

Similarly, the probability that ξ is within the interval $[x_1; x_2]$ can be obtained by $F_n(x_1) - F_n(x_2) = (x_2 - x_1)/n$. Then the β probability that ξ is outside this region is given by $\beta = 1 - (x_2 - x_1)/n$. In the following we suppose that the $[x_1; x_2]$ interval is symmetric to the \bar{x} sample mean. To obtain the empirical distributions of the test-variables we made 200 simulations for each of the five samples. The number of the simulated points were identical with those of the samples defined in Section 3.1.

We generated the fully random catalogs by Monte Carlo (MC) simulations of fully random GRB celestial positions and taking into account the BATSE sky-exposure function (Fishman et al. (1994), Meegan et al. (2000)).

Assuming that the point patterns obtained from the five samples, defined in Table 1, are fully random we calculated the probabilities for all the 13 test-variables selected in Section 3.2. Based on the simulated distributions we computed the level of significance for all the 13 test-variables and in all samples defined.

4 DISCUSSION OF THE STATISTICAL PROPERTIES

4.1 Significance of independent multiple tests

In Section 3.3 we calculated numerical significance for the tests assuming they were performed individually. The calculated significance levels are given in Table 2. In the reality, however, these figures would mean significance at a certain level if one performed only that single test. Assuming that all the single tests were independent the $P_n(m)$ probability that among n trials at least m will resulted significance only by chance at a certain level is given by the following equality:

$$P_n(m) = \sum_{k=m}^n P_k^n, \quad (1)$$

where P_k^n is the binomial distribution giving the probability of k successes among n trials:

$$P_k^n = \frac{n!}{k!(n-k)!} p^k (1-p)^{n-k}. \quad (2)$$

In the equation given above p means the probability that a single test has given significant result only by chance. It is easy to see that this equation resulted in $P_n(1) = 1 - (1-p)^n \approx np$ which gives a significance of $1 - np$ approximately instead of $1 - p$. It means e.g. that a single test resulted in $1 - p = 0.95$ significance is reduced to $1 - 0.95^{13} = 0.49$ if one performed $n = 13$ independent tests but only one resulted in $1 - p = 0.95$ significance.

Inspecting Table 2 listing the calculated numerical significance of single tests one can infer that *short1* sample has 4 tests with significance of $1 - p = 0.95$ ore more. Taking into account the calculations at the end of the previous paragraph, however, we have to emphasize that the calculated numerical significance, based on the individual probability distribution of the test-variables separately, does not have its original meaning. Significance refers to the certainty rejecting the null hypothesis on the basis of the bunch of tests as a whole. Applying Equation (1) with $m = 4$ and $n = 13$ one gets a significance of 99.69 %. Applying the same sequence of arguments to the *short2* sample one may get a figure of only 86.46 % ($m = 2$ and $n = 13$). In the case of the *intermediate*, *long1* and *long2* samples one can not get figures above the 95 % significance level.

One may have a serious concern, however, with the results obtained above. Namely, the basic requirement of the independence of the single tests is not fulfilled in our case. In the contrary, there are strong correlations between the test-variables in Table 2. In the next subsection we try to outline an approach which takes into account the correlations between the test-variables and overcomes this difficulty.

Table 2. Calculated significance levels for the 13 test-variables and the five samples. A **calculated numerical** significance greater than 95% is put in bold face.

Name	var	short1	short2	interm.	long1	long2
Cell area	A	36.82	29.85	94.53	79.60	82.59
Cell vertex (edge)	N_v	36.82	87.06	2.99	26.87	7.96
Cell chords	C	47.26	52.24	18.91	84.58	54.23
Inner angle	α_i	96.52	21.39	87.56	37.81	63.18
RF average	$\frac{4\pi A/P}{RF_{av}}$	65.17	99.98	33.83	10.95	86.07
RF homogeneity	$1 - \frac{\sigma(RF_{av})}{RF_{av}}$	19.90	24.38	58.71	55.72	32.84
Shape factor	A/P^2	91.04	94.03	90.05	55.22	63.68
Modal factor	$\sigma(\alpha_i)/N_v$	97.51	1.99	7.46	56.22	8.96
AD factor	$1 - \left(1 - \frac{\sigma(A)}{A}\right)^{-1}$	32.84	25.37	11.44	95.52	52.74
MST variance	$\sigma(L_{MST})$	52.74	38.31	22.39	13.93	59.70
MST average	L_{MST}	97.51	7.46	89.05	56.72	8.96
MST angle	α_{MST}	85.07	14.43	36.82	73.63	60.70
MFR spectra	$f(\alpha)$	95.52	96.02	98.01	73.63	36.32
Binomial test	(Eq. (1) with $p = 0.05$)	99.69	86.46	51.33	51.33	-
Squared Euclidean	distance	99.90	99.98	98.51	93.03	36.81

4.2 Evaluation of the joint significance levels

We assigned to every MC simulated sample 13 values of the test variables and, consequently, a point in the 13D parameter space. Completing 200 simulations in all of the subsamples we get in this way a 13D sample representing the joint probability distribution of the 13 test-variables. Using a suitable chosen measure of distance of the points from the sample mean we can get a stochastic variable characterizing the deviation of the simulated points from the mean only by chance. An obvious choice would be the squared Euclidean distance.

In case of a Gaussian distribution with unit variances and without correlations this would result in a χ^2 distribution of 13 degree of freedom. The test-variables in our case are correlated and have different scales. Before computing squared Euclidean distances we transformed the test-variables into non-correlated ones with unit variances. Due to the strong correlation between some of the test-variables we may assume that the observed quantities can be represented with non-correlated variables of less in number. Factor analysis (FA) is a suitable way to represent the correlated observed variables with non-correlated variables of less in number.

Since our test-variables are stochastically dependent following Wallet & Dussert (1998) we attempted to represent them by fewer non-correlated hidden variables supposing that

$$X_i = \sum_{j=1}^k a_{ij} f_j + s_i \quad i = 1, \dots, p; \quad k < p. \quad (3)$$

In the above equation X_i, f_j, s_i mean the test-variables ($p = 13$ in our case), the hidden variables and a noise-term, respectively. Equation (3) represents the basic model of FA.

After making some reasonable assumptions (Kendall & Stuart 1973), k can be constrained by the following inequality:

$$k \leq (2p + 1 - \sqrt{8p + 1})/2 \quad (4)$$

which gives $k \leq 8.377$ in our case.

Factor analysis is a common ingredient of professional statistical software packages (BMDP, SAS, S-plus, SPSS¹, etc). The default solution for identifying the factor model is to perform principal component analysis (PCA). We kept as many factors as were meaningful with respect to Equation (4). Taking into account the constraint imposed by Equation (4) we retained 8 factors. In this way we projected the joint distribution of the test-variables in the 13D parameter space into a 8D one defined by the non-correlated f_i hidden variables.

The f_j hidden variables in Equation (3) are non-correlated and have zero means and unit standard deviations. Using these variables we defined the following squared Euclidean distance from the sample mean:

$$d^2 = f_1^2 + f_2^2 + \dots + f_k^2 \quad (k = 8 \text{ in our case}) . \quad (5)$$

If the f_j variables had strictly Gaussian distributions Equation (5) would define a χ^2 variable of k degrees of freedom.

4.3 Statistical results and their interpretations

In addition to the significance obtained by the binomial test in Subsection 4.1 using the distribution of the squared Euclidean distances, defined by Equation (5), one can get further information whether a BATSE sample represented by a point in the parameter space of the test-variables deviates only by chance or it significantly differs from the fully random distribution.

In all categories (*short1*, *short2*, *intermediate*, *long1*, *long2*) we made 200, altogether 1000, simulations. We calculated the d^2 squared distances for all simulations and compared them with those of the BATSE samples in Table 1. Figure 4 shows a histogram of the simulated squared distances along with those of the BATSE samples. Full line represent a χ^2 distribution of $k = 8$ degree of freedom. Figure 4 clearly shows that the departures of samples *short1* and *short2* exceed all those of the simulated points. The probabilities, that these deviations are non-random, equal 99.9% and 99.98%, respectively.

¹ BMDP, SAS, S-plus, SPSS are registered trademarks

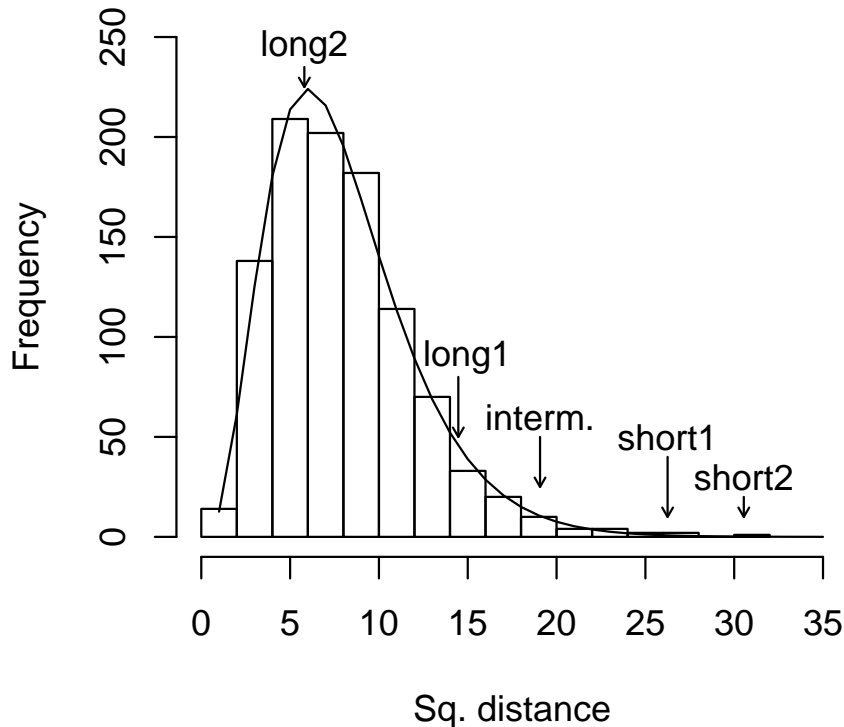


Figure 4. Distribution of the squared Euclidean distances of the simulated samples from the stochastic mean of the f_i hidden variables (factors) in the 8D parameter space. There are altogether 1000 simulated points. Full line marks a χ^2 distribution of 8 degree of freedom, normalized to the sample size. The distances of the BATSE samples are also indicated. The departures of samples "short1" and "short2" exceed all those of the simulated points. The probabilities, that these deviations are non-random, equal 99.9% and 99.98%, respectively.

The full randomness of the angular distribution of the long GRBs, in contrast to the regularity of the short and in some extent to the intermediate ones, points towards the differences in the angular distribution of their progenitors. The recent discovery of the afterglow in some short GRBs indicates that these events are associated with the old stellar population (Fox et al. 2005) accounted probably for the mergers of compact binaries, in contrast to the long bursts resulting from the collapse of very massive stellar objects in young star forming regions. The differences in progenitors reflects also the differences between the energy released by the short and long GRBs.

Unfortunately, little can be said on the physical nature of the intermediate class. The statistical studies (Horváth et al. (2006) and the references therein) suggest the existence of this subgroup - at least from the purely statistical point of view. Also the non-random sky distribution is occurring here. But its physical origin is fully open yet (Horváth et al. 2006).

5 SUMMARY AND CONCLUSIONS

We made additional studies on the degree of the randomness in the angular distribution of samples selected from the BATSE Catalog. According to the T_{90} durations and P_{256} peak fluxes of the GRBs in the Catalog we defined five groups: *short1* ($T_{90} < 2$ s & $0.65 < P_{256} < 2$), *short2* ($T_{90} < 2$ s & $0.65 < P_{256} < 2$), *intermediate* (2 s $\leq T_{90} \leq 10$ s & $0.65 < P_{256}$), *long1* ($T_{90} > 2$ s & $0.65 < P_{256} < 2$) and *long2* ($T_{90} > 10$ s & $0.65 < P_{256}$).

To characterize the statistical properties of the point patterns, given by the samples, we defined 13 test-variables based on the Voronoi tessellation (VT), Minimal spanning tree (MST) and Multifractal spectra. For all five GRB samples defined we made 200 numerical simulations assuming fully random angular distribution and taking into account the BATSE exposure function. The numerical simulations enabled us to define empirical probabilities for testing the null hypothesis, i.e. the assumption that the angular distributions of the BATSE samples are fully random.

Since we performed 13 single tests simultaneously on each subsamples the significance obtained by calculating it separately for each test can not be treated as a true indication for deviating from the fully random case. At first we supposed that the test-variables were independent and making use the binomial distribution computed the probability of obtaining significant deviation in at least one of the variables only by chance. In fact, some of the test-variables are strongly correlated. To concentrate the information on the non-randomness experienced by the test-variables, we assumed that they can be represented as a linear combination of non-correlated hidden factors of less in number. Actually, we estimated $k = 8$ as the number of hidden factors. Making use the hidden factors we computed the distribution of the squared Euclidean distances from the mean of the simulated variables. *Comparing the distribution of the squared Euclidean distances of the simulated with the BATSE samples we concluded that the short1, short2 groups deviate significantly (99.90%, 99.98%) from the fully randomness, but it is not the case at the long samples. At the intermediate group squared Euclidean distances also give significant deviation (98.51%).*

ACKNOWLEDGMENTS

This study was supported by OTKA grant No. T048870, by a Bolyai Scholarship (I.H.), by a Research Program MSM0021620860 of the Ministry of Education of Czech Republic, and

by a GAUK grant No. 46307 (A.M.). We are indebted to an anonymous referee for his valuable comments and suggestions.

REFERENCES

- Adami C., Mazure A., 1999, *A&AS*, 134, 393
- Aschwanden M.J., Parnell C.E., 2002, *ApJ*, 572, 1048
- Balázs L.G., Mészáros A., Horváth I., 1998, *A&A*, 339, 1
- Balázs L.G., Mészáros A., Horváth I., Vavrek R., 1999, *A&A Suppl.*, 138, 417
- Balázs L.G., Bagoly Z., Horváth I., Mészáros A., Mészáros P., 2003, *A&A*, 401, 129
- Barrow J.D., Bhavsar S.P., Sonoda D.H., 1985, *MNRAS*, 216, 17
- Bhavsar S.P., Lauer D.A., 1996, in Kafatos M.C., Kondo Y., eds, *Proc. IAU Symp.* 168, Examining the big bang and diffuse background radiations, Kluwer, Dordrecht, p. 517
- Bhavsar S.P., Splinter R.J., 1996, *MNRAS*, 282, 1461
- Bottorff M., Ferland G., 2001, *ApJ*, 549, 118
- Briggs M., 1993, *ApJ*, 407, 126
- Casuso E., Beckman J., 2002, *PASJ*, 54, 405
- Célérier M.N., Thieberger R., 2001, *A&A*, 367, 449
- Chappell D., Scalo J., 2001, *ApJ*, 551, 71
- Cline D.B., Matthey C., Otwinowski S., 2000a, in Kippen R.M., Malozzi R.S., Fishman G.J., eds, *AIP Conf. Proc.*, *Gamma-Ray Bursts: 5th Huntsville Symp.*, Melville, New York, p. 97
- Cline D.B., Matthey C., Otwinowski S., 2000b, *ApJ*, 527, 827
- Coles P., Barrow J.D., 1990, *NMRAS*, 244, 557
- Coles P., 1991, *Nature*, 349, 288
- Datta S., 2003, *A&A*, 401, 193
- Diggle P.J., 1983, *Statistical Analysis of Spatial Point Patterns*, Academic Press, London
- Doroshkevich A.G., Gottlöber S., Madsen S., 1997, *A&A Suppl.*, 123, 495
- Doroshkevich A.G., Turchaninov V., 2001, in Banday A.J., Zaroubi S., Bartelmann M., eds, *Proc. 'Mining the Sky' MPA/ESO/MPE Workshop*, Springer-Verlag, p.283
- Elmegreen B.G., 2002, *ApJ*, 564, 773
- Fishman G.J., Meegan C.A., Wilson R.B., et al., 1994, *ApJS* 92, 229
- Fox D.B., Frail D.A., Price P.A., Kulkarni S.R., Berger E., et al., 2005, *Nature*, 437, 845

- Gaite J., Manrubia S.C., 2002, MNRAS, 335, 977
- Giraud E., 2000, ApJ, 544, L41
- Hakkila J., Haglin D.J., Pendleton G.N., Mallozzi R.S., Meegan C.A., Roiger R.J., 2000, ApJ, 538, 165
- Hakkila, J., et al., 2003, ApJ, 582, 320
- Horváth I., 1998, ApJ, 508, 757
- Horváth I., 2002, A&A, 392, 791
- Horváth I., Balázs L.G., Bagoly Z., Ryde F., Mészáros A., 2006, A&A, 447, 23
- Icke V., van de Weygaert R., 1991, QJRAS, 32, 85
- Ikeuchi S., Turner E.L., 1991, MNRAS, 250, 519
- Irwin J.A., Widrow L.M., English J., 2000, ApJ, 529, 77
- Kawaguchi T., Mineshige S., Machida M., Matsumoto R., Shibata K., 2000, PASJ, 52, L1
- Kendall, M.G., & Stuart, A. 1973, *The Advanced Theory of Statistics*, Charles Griffin & Co. Ltd., London & High Wycombe
- Kouveliotou, C., et al., 1993, ApJ, 413, L101
- Kruskal J.B., 1956, Proc. Am. Math. Soc., 7, 48
- Krzewina L.G., Saslaw W.C., 1996, MNRAS, 278, 869
- Magliocchetti M., Ghirlanda G., Celotti A., 2003 MNRAS, 343, 255
- Litvin V.F., Matveev S.A., Mamedov S.V., Orlov V.V., 2001, Pis'ma v Astron. Zhurnal, 27, 489
- Meegan C.A. et al., 2000, BATSE Gamma-Ray Bursts Catalog, <http://gammaray.msfc.nasa.gov/batse/grb/catalog>
- Mészáros A., Bagoly Z., Vavrek R., 2000a, A&A, 354, 1
- Mészáros A., Bagoly Z., Horváth I., Balázs L.G., Vavrek R., 2000b, ApJ, 539, 98
- Mészáros A., Štoček J., 2003, A&A, 403, 443
- Mészáros P., 2006, Rep. Prog. Phys., 69, 2259
- Mukherjee, S., et al. 1998, ApJ, 508, 314
- Murtagh F., Heck A., 1987, *Multivariate data analysis*, Astrophysics and Space Science Library, Dordrecht: Reidel
- Paladin G., Vulpiani A., 1987, Physics Reports, 156, 1
- Pan J., Coles P., 2000, MNRAS, 318, l51
- Pan J., Coles P., 2002, MNRAS, 330, 719
- Pásztor L., Tóth L.V., 1995, in Shaw R.A., Payne H.E., Hayes J.J.E., eds, ADASS IV, ASP

- Conf. Ser., Vol. 77, p. 319
- Pendleton C.N., Paciesas W.S., Briggs M.S., et al., 1997, *ApJ*, 489, 175
- Press W.H., Flannery B.P., Teukolsky S.A., Vetterling W.T., 1992, *Numerical Recipes*, Cambridge University Press, Cambridge
- Prim R.C., 1957, *Bell Syst. Techn. Journ.*, 36, 1389
- Ramella M., Boschin W., Fadda D., Nonino M., 2001, *A&A*, 368, 776
- Selman F.J., Melnick J., 2000, *ApJ*, 534, 703
- Semelin B., Combes F., 2002, *A&A*, 387, 98
- Springel V., White, S.D.M., Jenkins A., Frenk C. S., Yoshida N., Gao L., et al., 2005, *Nature*, 435, 629
- Stoyan D., Stoyan H., 1994, *Fractals, Random Shapes and Point Fields*, Wiley J. & Sons, New York
- Subba Rao M.U., Szalay A.S., 1992, *ApJ*, 391, 483
- Tanvir, N.R., Chapman, R., Levan, A.J., Priddey, R.S., 2005, *Nature*, 438, 991
- Tatekawa T., Maeda K., 2001, *ApJ*, 547, 531
- Tikhonov A.V., 2002, *Astrophysics*, 45, 79
- Vavrek R., Balázs L.G., Epchtein N., 2001, in Montmerle T., André P., eds, 'From Darkness to Light' ASP Conf. Ser., Vol. 243, p. 149
- Voronoi G., 1908, *J. Reine Angew. Math.*, 134, 198
- Wallet, F., Dussert C., 1997, *J. theor. Biol.*, 187, 437
- Wallet, F., Dussert C., 1998, *Europhys. Lett.*, 42, 493
- van de Weygaert R., 1994, *A&A*, 283, 361
- Yahagi H., Mori M., Yoshii Y., 1999, *ApJS*, 124, 1
- Zhang B., Mészáros P., 2004, *IJMPA*, 19, 2385
- Zaninetti L., 1995, *A&AS*, 109, 71